Particle Accelerators, 1992, Vols. 37–38, pp. 141–149
Reprints available directly from the publisher
Photocopying permitted by license only

3D SIMULATIONS OF AXIALLY CONFINED HEAVY ION BEAMS IN ROUND AND SQUARE PIPES†

D. P. GROTE and A. FRIEDMAN

Lawrence Livermore National Laboratory, Livermore, CA 94550

I. HABER

U.S. Naval Research Laboratory, Washington DC 20375.

(Received 3 December 1990)

We have been using the 3d Particle-in-cell (PIC) code WARP6[1] to model the behavior of beams in a heavy ion induction accelerator; such linacs are candidates for an ICF driver. Improvements have been added to the code to model an axially confined beam using comoving axial electric fields to simulate the confining "ears" applied to the accelerating pulses in a real system. We have also added a facility for modeling a beam in a round pipe, applying a capacity matrix to each axial Fourier mode in turn. These additions are described along with results, such as the effect of pipe shape on the beam quality degradation from quadrupole misalignments.

1 INTRODUCTION

WARP6 is a three dimensional electrostatic particle-in-cell code which incorporates an acceleration lattice. Its purpose is to model the propagation and acceleration of an ion beam. The particle-in-cell description includes in the force equation the proper non-linear self-consistent electric fields of the high-current beams used in heavy ion fusion applications.

Until now, the WARP6 could study the long time evolution only of infinitely long beams, making the assumption of periodicity. Finite beams exhibited free expansion longitudinally due to both thermal forces and space charge forces. Beams run with an axial (z) velocity "tilt" (head-to-tail gradient) were initially compressed, but expansion soon took over again, blowing up the beam. Models were needed for tapered-end beams, and for fields to confine those beams. In the first section, we describe the finite beam model we have developed.

The code works in Cartesian coordinates, allowing fast Fourier transforms to be used in solving Poisson's equation and making particle deposition onto the grid straightforward. The fields most readily solved for are thus those of a beam in a square pipe. In the second section below, we describe our round-pipe model. We then

† Work performed in part under the auspices of the U.S. Dept. of Energy by Lawrence Livermore National Laboratory under contract W-7405-ENG-48.

compare simulations in square and round pipes; the latter are more common in actual accelerators, but modeling them is computationally more expensive.

2 FINITE BEAMS AND CONFINING FIELDS

In our model, a finite beam has a constant line charge density in the middle of the beam, and a tapered line charge density in the ends, which in our runs to date comprise typically one-half to one-fifth of the total beam length. We use the formulas derived by Neufffer for the axial position and velocity distribution to construct a taper with a parabolic fall-off in line charge density.[2] We assume that $I/\varepsilon_\perp$ is constant in the taper. Here, I is the beam current and $\varepsilon_\perp = \varepsilon_{xx'} = \varepsilon_{yy'}$ is the transverse emittance, x and y are the transverse coordinates, y being in the vertical direction. This corresponds to constant tune depression, or constant number density, and gives a cigar-shaped beam. It allows us to use the same envelope solution everywhere along the beam to match it to the AG lattice, but scaled by the parabolic taper in the ends. The transverse distribution function in the ends is the same as in the middle of the beam, either semiGaussian (uniform in space, Gaussian in velocity), or K-V[3]. The number density is constant everywhere in the beam. See Figure 1.

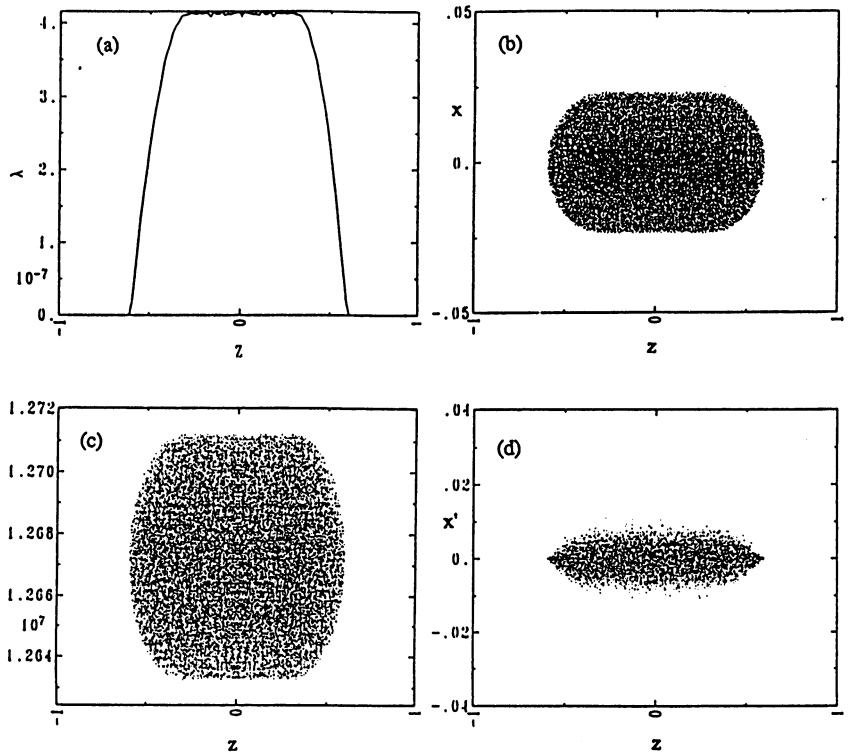

FIGURE 1 Line charge density and particle plots showing the initial shape of the finite beam. (a) line charge density, (b) x versus z, (c) v_z versus z, and (d) x' versus z ($x' = v_x/v_z$).

The confining fields consist of an axial electric field, constant in the transverse plane but varying in z, which is continually applied to the beam. This field moves along with the beam and is applied at every time step. The axial confining field consists of two parts. The first is the negative of the initial axial electric self-field on axis in the tapers which extends slightly into the middle section. This is a non-linear function of z because the beam radius is not constant; thus the "g-factor" varies with z, in contradiction to the assumption of Neuffer's paper. The second is an electric field, which is needed to counteract the thermal expansion. The expression derived by Neuffer is used. It is a linear electric field that starts at the ends of the straight part of the beam. For the high-current, low-axial-emittance beams useful for heavy ion fusion, the second part is much smaller. A comparison of the confining axial field and the axial self-field is shown in Figure 2.

Many runs have been carried out using the axial confinement model; we summarize some of them here. See Table 1 for the parameters of the runs described. Run number one, initialized with the tapers half the total length of the beam, uniform focusing, and cold in z, was run for 120 m. Another, run number two, was started off with the thermal v_z the same as the thermal $v_\perp$, the other parameters being the same, and was run for 60 m. Run number three was taken the farthest, to 210 m. It used magnetic quadrupole focusing with a tune depression of 60° and 20° (phase advance per lattice

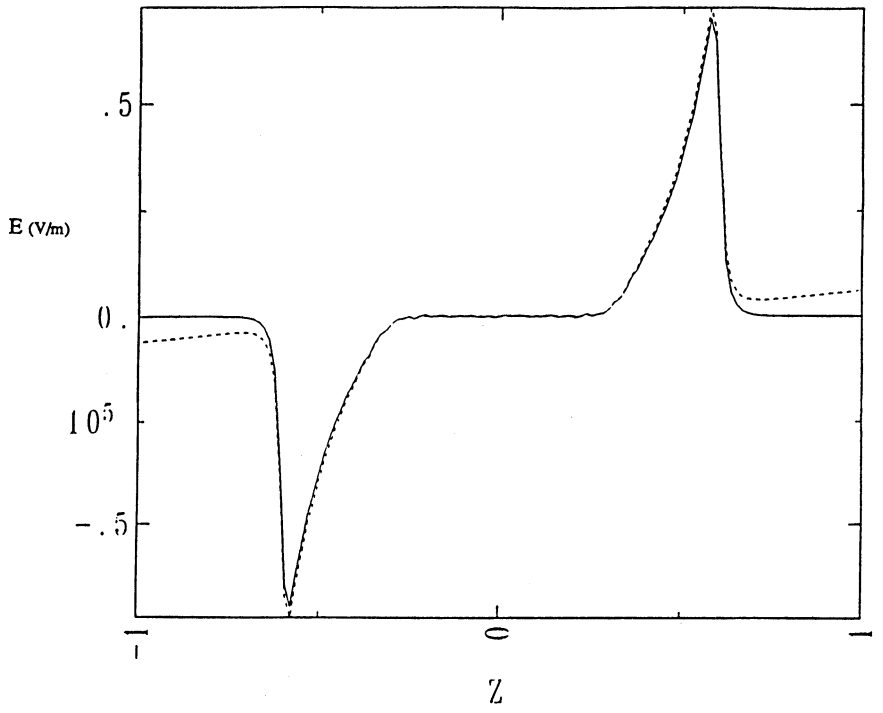

FIGURE 2 Comparison of the applied confining axial field (negative of dotted line) with the axial self field (solid line). The difference is the linear part which offsets axial the thermal expansion.

TABLE 1

Run name focusing[1]	1 Uniform	2 Uniform	3 Quadrupole	4 Quadrupole	5 Quadrupole	6 Quadrupole
Tune[2] (Phase advance per lattice period)	60° to 20°	60° to 20°	60° to 20°	60° to 55°	60° to 20°	60° to 20°
a_0[3] (cm)	2.34	2.34	3.05	1.87	3.05	3.05
b_0[4] (cm)	2.34	2.34	1.88	1.12	1.88	1.88
Current (amps)	5.22	5.22	5.22	0.343	5.22	5.22
Wall location) (cm)	±5	±5	±9	±9	±9	5[5]
Beam length (m)	1.2	1.2	1.2	1.2	1.2	1.2
Taper len Total len	1/2	1/2	1/2	1/5	1/5	1/5
Initial RMS Vz (m/s)	50.0	2×10^4	4×10^3	2×10^3	2×10^4	2×10^4
Run length (m)	120	60	210	144	18	18
Notes						Round pipe

All of the runs had the following parameters; $\varepsilon_\perp = 16$ mm-mrad, $V_{beam} = 1.27 \times 10^7$ m/s, ~50000 simulation particles.

[1] Uniform focusing means a radial electric field continuously applied to a cylindrical beam. Quadrupole focusing means strong focusing with magnetic quadrupoles. The quadrupole focusing lattice is periodic with periodicity of 1.2 m. It is a FODO arrangement with magnets 0.2 m long and a 0.4 m drift space.

[2] (Undepressed) to (depressed); for uniform focused runs, the phase advance is measured as if there were a 1,2 m period.

[3] The maximum initial semi-axis of the beam.

[4] The minimum initial semi-axis of the beam.

[5] The radius of the pipe.

period), and the thermal v_z almost a factor of 10 less than the thermal $v_\perp$. All of these runs were well-behaved. The axial spreading was much less than 1% of the beam length, and less than 10 out of about 50 000 particles were lost out the ends. Also, the transverse emittance remained roughly constant in time over much of the beam, with no greater than 10% fluctuations; there was no net transverse heating in the straight section, and only heating by a factor of 1.5 to 2 in the tapered ends, signifying that the tapered ends were not in equilibrium. Contour plots of the line charge density λ, versus time and z, and overlay plots of λ versus z at various times, are shown for run number 2 in Figure 3(a).

Run number three is shown in more detail in Figures 4 and 5. Particle plots of x and y versus z at the start of the run and at the end of the run are shown in Figure 4. The only differences are the edge of the beam which is ragged after the run, and the few particles that have escaped the head and tail of the beam. In Figure 5, the transverse emittance, $\varepsilon_{xx'}$, at four places in the beam is shown. The only one that shows growth is the one near the tip of the taper. Figure 5 also shows the z thermal energy. The initial rapid rise is an equilibration effect common to runs initialized colder in z than in x and y, which we believe to be physical[4]. The subsequent slower rise is the result of numerical heating common to particle codes; it can be reduced by increasing the number of particles. The z thermal energy and the transverse emittance in the tapers are the only parameters that show any significant change.

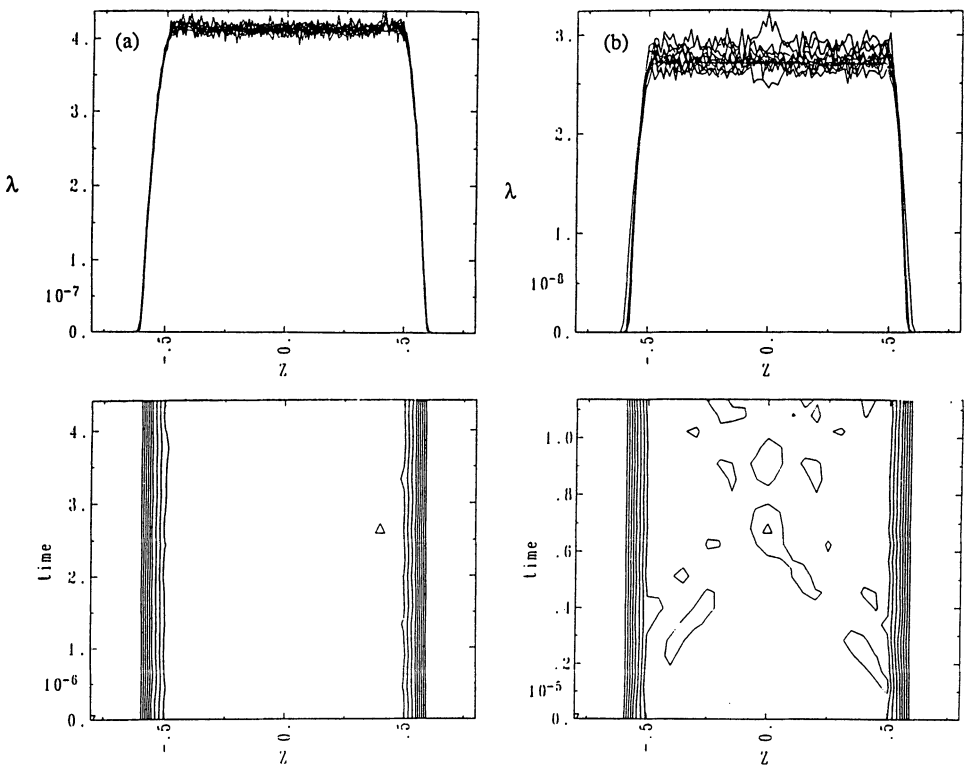

FIGURE 3 Plots of the line charge density for two runs. (a) Uniform focusing run with the thermal v_z the same as the thermal $v_\perp$ (run number 2). Overlay of λ versus z at several time steps and a contour of λ versus z versus time. (b) Longitudinally emittance dominated (run number 4), with same overlay and contour plots.

A run that was emittance-dominated in the longitudinal direction was also made (number 4 in Table 1). The tune was depressed only to 55°, and the thermal v_z was several times larger than the thermal $v_\perp$. The model for the confining field was not accurate enough for this case; sounds waves were launched into the center of the beam. See Figure 3(b).

The confining field is intended to model the confining fields used in a real accelerator. In the latter, the confining field is applied only at the acceleration gaps, along with the accelerating fields; this is done by applying "ears" to the accelerating pulses. The true intermittently applied field is more difficult to derive since it must also compress the beam slightly to account for the free expansion between accelerating gaps. This more complicated field will have space and time dependence, and will require minor code development. Our initial efforts at modelling intermittent application of the confining force did not use a carefully tuned field, and led to large fluctuations; we are currently examining this area.

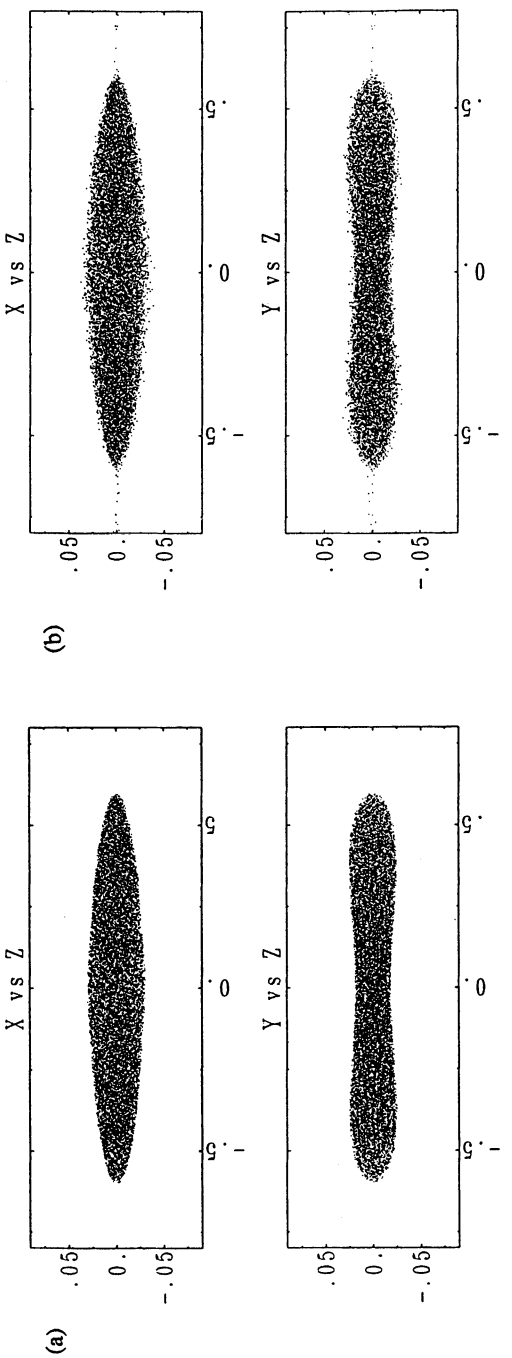

FIGURE 4 Particle plots of x and y versus z, from run number 3: (a) at the beginning of the run and (b) at the end of the run.

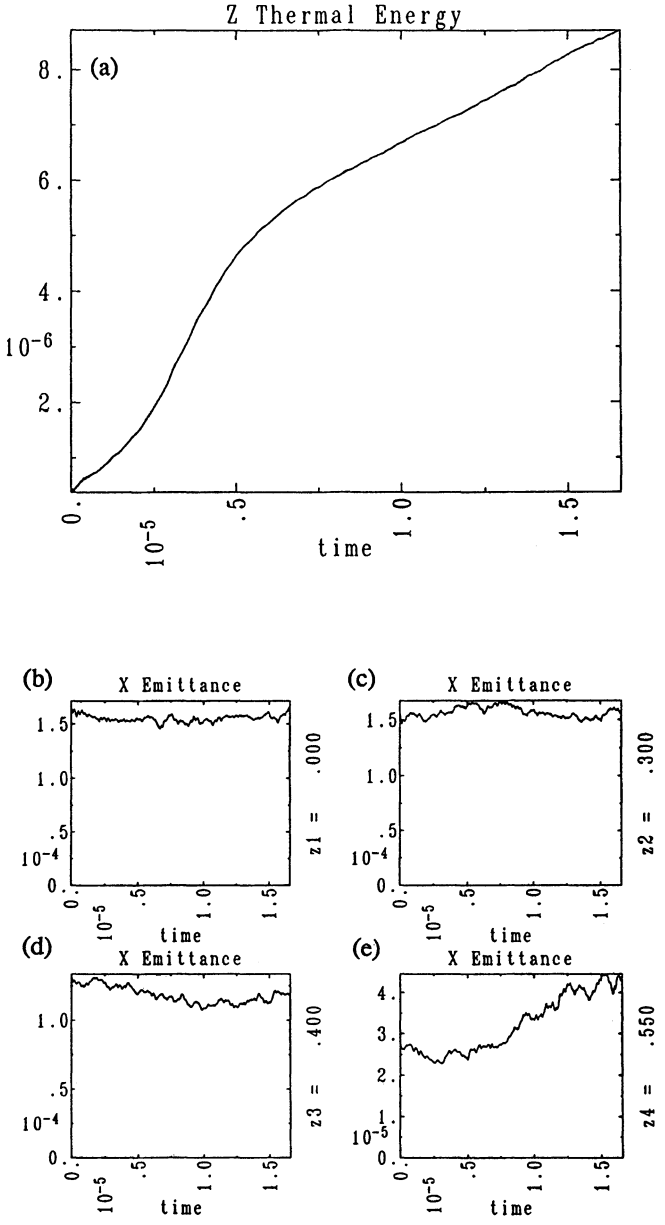

FIGURE 5 History plots from run number 3: (a) z thermal energy shows significant growth. The initial rise results from what appears to be a collective equilibration between longitudinal and transverse thermal energy, which we believe to be physical; the slower final rise is due to numerical heating associated with the nonphysically small number of particles. The x emittance shows no growth in (b) the middle of the beam, (c) the end of the straight section, and (d) partway into the taper, but does grow in (e) the end of the taper. The y emittance behaves similarly.

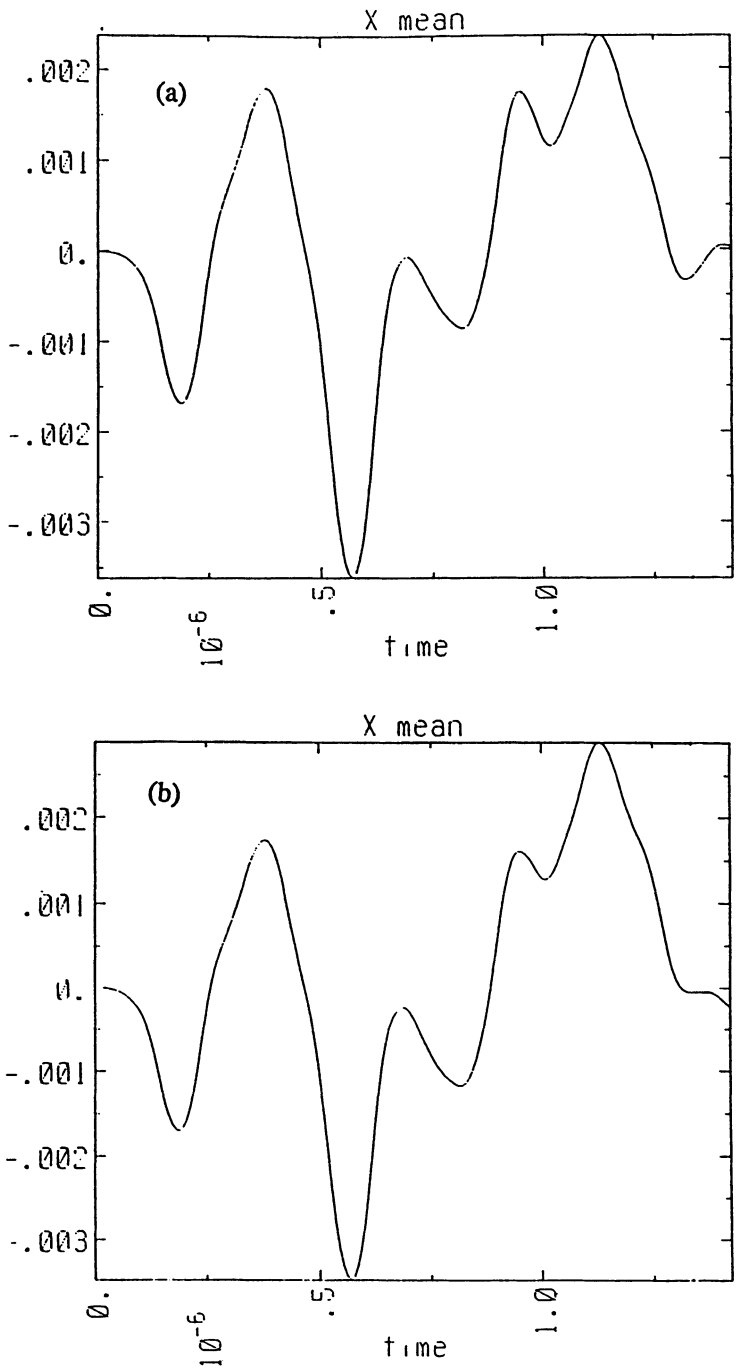

FIGURE 6 Comparisons of the x mean of the center of a beam versus time in offset quadrupole with 5 cm round and square pipes: (a) square pipe (run number 5), (b) round pipe (run number 6).

3 ROUND AND SQUARE PIPES

To calculate the fields in a round pipe, the capacity matrix method[5] is employed. For an infinitely long round pipe, calculation and storage can be reduced by taking advantage of symmetries. For any infinite pipe, the axial Fourier modes are independent, allowing a separate matrix for each axial mode. This saves substantial storage and time, since the capacity matrix elements relating the axial modes to each other all vanish. In the transverse plane, a circle inscribed in a square has an eightfold symmetry. This reduces the computation needed to calculate the capacity matrices and the memory needed to store them by almost a factor of eight. The necessary points on the bounding conductor are placed on a circle independent of the grid, thereby avoiding a jagged circle. This allows a smaller number of points for the same accuracy. The matrices are calculated once at the beginning of the run, and applied at each time step.

Several axially confined beam runs were done with randomly offset quadrupole magnets, representing alignment errors. The offsets were all in the transverse plane, with x and y RMS values of 1 mm. The offsets move the beam off center; a beam with maximum radius of 3 cm is shifted, at most 3 mm off axis in x and y when followed over 18 m. Runs with the walls at ± 5 cm and ± 7 cm were done with both round and square pipes (see runs 5 and 6 in Table 1). The runs had a tune depression of 60° to 20°, with the thermal v_z the same as the thermal $v_\perp$. For either wall distance, there was little effect from the shape of the pipe, as shown in Figure 6; the fluctuations in emittance and beam centroid appear to be quite insensitive to the pipe shape. There was no net emittance growth in either run.

REFERENCES

1. A. Friedman, D. A. Callahan, D. P. Grote, A. B. Langdon, and I. Haber, in Proceedings of the Conference on Computer Codes and the Linear Accelerator Community, edited by R. K. Cooper and K. C. D. Chan (Los Alamos, NM. 1990).
2. David Neuffer, "Longitudinal motion in high current ion beams—a self-consistent phase space distribution with an envelope equation," *IEEE Trans. Nucl. Sci.* **NS-26** 3 (June 1979) 3031.
3. I. M. Kapchinskij and V. V. Vladimirskij, "Limitations of proton beam current in a strong focusing linear accelerator associated with the beam space charge". In *Proceedings of the Second International Conference on High Energy Accelerators* (1959) pp. 274–288.
4. A. Friedman *et al.*, these Proceedings.
5. R. W. Hockney and J. W. Eastwood, *Computer Simulations Using Particles*, Adam Hilger, (Bristol 1988), p. 215.